Subpicosecond pump-probe absorption of the hydrated electron: Nonlinear response theory and computer simulation

S. Bratos, J.-Cl. Leicknam, D. Borgis, and A. Staib*
Laboratoire de Physique Théorique des Liquides, Université Pierre et Marie Curie, Case Courrier 121, 4 Place Jussieu, 75252 Paris Cedex 05, France
(Received 23 September 1996)

A theory is presented to study the subpicosecond transient absorption of the hydrated electron. Applicable in equilibrium conditions, this theory is a statistical theory using a correlation function approach to the nonlinear optical process involved. Four-time correlation functions of the electric moment and of the incident electric fields are employed extensively. An analytical expression for the transient signal is obtained; both coherent and incoherent electric fields are considered. The parameters of this theory are evaluated by means of a mixed quantum-classical molecular-dynamics simulation; water molecules are assumed to be rigid. The hydrated electron is described in terms of floating Gaussian orbitals; the solvent polarizability is accounted for in a self-consistent way. Theoretical time- and frequency-resolved spectra are compared with experiment. Nonmonotonic behavior of spectral transients is attributed to a competition between thermic and nonthermic subbands of the signal. Most of the spectral evolution is achieved in 20–30 fs by the fast inertial response of the solvent. [S1063-651X(97)05506-2]

PACS number(s): 82.20.Wt

I. INTRODUCTION

Since its discovery in 1962, the hydrated electron e_{aq}^- has been extensively studied by a number of authors. This chemical species plays a significant role in solution photochemistry, the radiation chemistry of water and in electron-transfer reactions. It is omnipresent in irradiated aqueous systems. The nature of its coupling to the solvent fluctuations is of paramount importance in many chemical processes. It is thus not surprising that there has been an intense experimental effort in this field. For textbooks and reviews covering the subject, see, e.g., Refs. [1,2].

During the last decade, interest shifted to the study of the pico- and femtosecond kinetics of e_{aq}^-; two sorts of experiment were set up. (i) The electron is injected into water by a two-photon excitation of H_2O at 310 nm [3–5], or by pumping at other wavelengths [6,7]. The early-time dynamics are explored immediately after the photodetachment, the electron still being within the reach of Coulomb forces due to the OH_2^+ ion. The motions of the prehydrated electron may be explored in this way. (ii) The experiment is realized several nanoseconds after the injection of e^- [8–10]. The electron is then trapped into a solvent cavity by the forces emanating from the neutral H_2O molecules. The behavior of a fully hydrated electron in thermal equilibrium can be examined by this technique.

The theory of electron hydration was first elaborated on a semimacroscopic level. The electron was treated as a particle in a dielectric cavity containing, or not, water molecules of the first coordination shell; see, e.g., Refs. [11,12]. The stationary absorption of e_{aq}^- was first studied in this way. On the contrary, modern work is entirely microscopic; the following directions of research were explored. (i) The equilibrium properties of an excess electron in water at room temperature was simulated using the Feynman path-integral formulation of quantum-statistical mechanics [13–16]. It was shown that the excess electron forms a cavity with a radius of 2.1–2.2 Å, and that the optical absorption band is due to a strongly allowed $1s \rightarrow 2p$ transition. (ii) Relaxation dynamics and transport behavior of the excess electron in clusters and in bulk water were studied with the help of an adiabatic simulation method [17–23]. The solvent evolves classically and the electron is constrained to a specified quantum state; the golden rule then allows the evaluation of nonadiabatic transition rates. The population relaxation was attributed to the breakdown of the Born-Oppenheimer approximation. It was also shown that the solvent relaxes through two time scales: a fast scale of the order of 20–30 fs associated with molecular librations, and a less well identified slower scale of the order of 100–200 fs. The calculated population relaxation times are the order of 250 fs. (iii) A new algorithm for quantum-dynamical simulation of a mixed classical-quantum system was introduced to calculate the nonadiabatic transition rates directly [24–30]. Important methodological innovations were required for that purpose. The role played by the solvent flexibility in the dynamics of solvation was also investigated; its effect on various relaxation times was found to be unexpectedly large. The existence of two time scales in the solvent relaxation, brought out by adiabatic simulations, was reconfirmed. On the contrary, the survival probability of the excited state, of the order of 700 fs, was larger than in adiabatic calculations. Combining data from theory and experiment, an important body of knowledge was built up.

In spite of this progress, the theoretical reconstruction of transient absorption spectra remained uneasy. The reason is that the interplay between a molecular system and a laser-produced electric field cannot be described by computer simulations alone, and methods of nonlinear physics must be adopted; see, e.g., Refs. [31–38]. This objective had not yet

*Present address: Institut für Theoretische Chemie, Universität Düsseldorf, Universitätsstrasse 1, D-40225 Düsseldorf, Germany.

been attained, but simplified models were elaborated to compare calculations and experiment. For example, nonequilibrium experiments were simulated by introducing an electron 2 eV above the ground level [27]. Alternatively, equilibrium experiments were analyzed by selecting from the ground-state trajectories configurations in resonance with the incident laser field [30]. The matrix elements $\mathbf{r}_{if}(t) = \langle \Psi_i(t) | \mathbf{r} | \Psi_f(t) \rangle$ were then calculated for each final state, and the absorption spectrum computed as a sum over final states. These models, although useful, cannot provide a complete picture. For example, they do not account for the presence of the initial, pump prepared and coherently excited packet of states. Moreover, as the pump and probe fields overlap at short times, the response of the system cannot be a linear response to the probe field alone. The above models are thus not satisfactory for time delays below 200 fs. A statistical theory of pump-probe absorption of e^-_{aq} is thus necessary.

The purpose of this paper is to present a statistical theory of this kind for a hydrated electron in equilibrium conditions. It employs the correlation function approach to nonlinear optics. An analytical expression for the transient signal is given for both time- and frequency-resolved spectra. The parameters of the theory are determined by quantum-mechanical simulations in which the hydrated electron is described by means of floating Gaussian orbitals, and the polarizability effects are accounted for in a self-consistent way. For a preliminary statistical analysis of this problem, see Ref. [38].

II. STATISTICAL DESCRIPTION

A. Basic formulas

The system under consideration is a sample of liquid water in thermal equilibrium, containing one extra electron [8–10]. It mimics a hydrated electron embedded in its local structure, and is globally charged. A strong pump pulse of frequency Ω_1 produces a transition between the lowest quantum states of the hydrated electron, and a weak probe pulse of frequency Ω_2, delayed by a time τ, explores its return to the ground state. The duration of the two pulses is of the order of 100 fs and their spectral width of the order of $350\ \mathrm{cm}^{-1}$. The measured quantity is the signal $S(\Omega_1,\Omega_2,\tau)$, defined as the total probe absorption $W(\Omega_1,\Omega_2,\tau)$ in the presence of the pump minus the probe absorption $W(\Omega_2)$ in the absence of the pump. Other relevant quantities are the electric field $\mathbf{E}_1$ of the pump, the electric field $\mathbf{E}_2$ of the probe, and the total electric field $\mathbf{E} = \mathbf{E}_1 + \mathbf{E}_2$. The vectors $\mathbf{E}_1$ and $\mathbf{E}_2$ are supposed to be parallel to each other; the perpendicular polarization experiment, although already realized [10], is not considered in this paper. Finally, $\mathbf{M} = \Sigma_i q_i(\mathbf{r}_i - \mathbf{r}_0)$ is the electric moment of the system. As the latter is globally charged, $\mathbf{M} \equiv \mathbf{M}(\mathbf{r}_0)$ depends on the choice of the reference point $\mathbf{r}_0$.

An important feature of this problem is the spatial variation of the incident electric fields within the experimental cell. In fact, the wavelength λ is much smaller than cell dimensions: the field variation inside the cell must be considered. However, molecular motions are monitored only over distances that are small with respect to λ. Under these conditions, the spatial variation of $\mathbf{E}_1, \mathbf{E}_2, \mathbf{E}$, can be accounted for by replacing the real system by a large number of replicas. They all experience a spatially constant electric field, but this field is different in each replica. The final result is obtained by averaging over the replicas. This procedure is of common use in the field; compare with Refs. [32,36].

The signal $S(\Omega_1,\Omega_2,\tau)$ being defined in terms of power $\mathcal{P}$ dissipated by unit volume of the liquid sample, introducing the Joule law $\mathcal{P} = \mathcal{J}\mathcal{E}$ seems natural. In this problem, $\mathcal{E}$ is the electric field $\mathbf{E}_2$ of the probe. Likewise, $\mathcal{J}$ is the current density $\mathbf{J}$ in the presence of the pump field; it is expressible in terms of the average electric moment $\langle \mathbf{M} \rangle$. The corresponding quantities in the absence of $\mathbf{E}_1$ are $\mathbf{J}_0$ and $\langle \mathbf{M} \rangle_0$. Then, designating by $\mathcal{V}$ the volume of the liquid sample, one finds

$$\mathcal{V}\mathcal{J} = \left\langle \sum_i q_i \mathbf{v}_i \right\rangle = \frac{d}{dt} \left\langle \sum_i q_i \mathbf{r}_i \right\rangle = \frac{d}{dt} \left\langle \sum_i q_i (\mathbf{r}_i - \mathbf{r}_0) \right\rangle = \frac{d}{dt} \langle M \rangle,$$

$$\mathcal{S} = W - W_0 = \int_{-\infty}^{\infty} dt \left[\mathbf{E}_2 \frac{d}{dt} (\langle M \rangle - \langle M \rangle_0) \right] = -\int_{-\infty}^{\infty} dt\ \dot{E}_2 [\langle M \rangle - \langle M \rangle_0], \tag{1}$$

where M, M_0 are the components of $\mathbf{M}$, $\mathbf{M}_0$ in the polarization direction. For the choice of the reference point $\mathbf{r}_0$, see below.

Explicit calculations require the knowledge of the Hamiltonian H of the system. It can conveniently be presented as a sum of two parts, a nonperturbed field-free part H^0 and a perturbation V due to the incident field. If $\mathbf{r}$ denotes the location of a given replica in the experimental cell, $V = V(\mathbf{r},t) = V(\mathbf{E}(\mathbf{r},t)) \equiv V(\mathbf{E})$. Then recalling that $\mathbf{E}$ is spatially constant within a replica, one can write

$$H(\mathbf{r},t) = H^0 + V(\mathbf{r},t),$$

$$V(\mathbf{E}) = \sum_i q_i \phi(\mathbf{r}_i), \quad \phi(\mathbf{r}_0) - \phi(\mathbf{r}_i) = \int_{\mathbf{r}_0}^{\mathbf{r}_i} d\mathbf{s}\ \mathbf{E} = (\mathbf{r}_i - \mathbf{r}_0)\mathbf{E}, \tag{2}$$

$$V(\mathbf{E}) = \left(\sum_i q_i \right) \phi(\mathbf{r}_0) - \left(\sum_i q_i (\mathbf{r}_i - \mathbf{r}_0) \right) \mathbf{E} = -\mathbf{M} \cdot \mathbf{E}. \tag{3}$$

For convenience, the zero of the potential $\phi(\mathbf{r})$ was chosen at $\mathbf{r} = \mathbf{r}_0$. Equations (2) and (3) define the Hamiltonian H, which was desired. The dynamical variable coupling a charged molecular system and an electric field is its electric moment with respect to the zero point of the electric potential ϕ. If the reference point $\mathbf{r}_0$ of Eq. (1) is chosen in the

same way, the calculations involve a single dynamical variable. This convention will be adhered to in what follows; it simplifies the theory considerably.

Further developments require the knowledge of the density operator $\rho=\rho(\mathbf{r},t)$ associated with the Hamiltonian of Eq. (2). This quantity may be evaluated by treating von Neumann's equation perturbatively up to third order in E. In fact, the first nonvanishing contribution to the pump-probe signal $S(\Omega_1,\Omega_2,\tau)$ is of this order. The procedure has been described repeatedly in the literature and will not be redescribed here; see, e.g., Refs. [32,39,40]. Then, if the $\mathbf{r}_0$ dependence of M is no longer indicated, one finds

$$\frac{\partial}{\partial t}\rho(\mathbf{r},t)=\frac{i}{\hbar}[H(\mathbf{r},t),\rho(\mathbf{r},t)], \tag{4}$$

$$M^{(3)}(\mathbf{r},t)=\mathrm{Tr}[\rho^{(3)}(\mathbf{r},t)M(\mathbf{r},t)]=\int_0^\infty\int_0^\infty\int_0^\infty d\tau_1 d\tau_2 d\tau_3[E(\mathbf{r},t-\tau_1)E(\mathbf{r},t-\tau_1-\tau_2)E(\mathbf{r},t-\tau_1-\tau_2-\tau_3)]$$

$$\times\frac{i^3}{\hbar^3}\,\mathrm{Tr}(M\,\exp(-iL\tau_1)[M,\exp(-iL\tau_2)[M,\exp(-iL\tau_3)[M,\rho_{\mathrm{eq}}]]]), \tag{5}$$

where $\rho=\Sigma_n\rho^{(n)}$, $L=[H^{(0)},\ ]/\hbar$ is the nonperturbed Liouville operator of the liquid system, and ρ_{eq} the equilibrium density matrix. Developing the commutators [,], eight terms appear. They may be handled by (i) utilizing the invariance of the trace operation under a cyclic permutation of factors and (ii) noticing that the resulting terms are all stationary time-dependent functions.

The final expression for the signal $S(\Omega_1,\Omega_2,\tau)$ can be obtained by substituting Eq. (5) into Eq. (1), and by using the above arguments. If one proceeds in this way, the following result may be reached:

$$S(\Omega_1,\Omega_2,\tau)=(2/\hbar^3)\mathrm{Im}\Bigg\{\int_{-\infty}^\infty\int_0^\infty\int_0^\infty\int_0^\infty dt\ d\tau_1 d\tau_2 d\tau_3\langle\dot{E}_2(\mathbf{r},t)E(\mathbf{r},t-\tau_3)E(\mathbf{r},t-\tau_3-\tau_2)E(\mathbf{r},t-\tau_3-\tau_2-\tau_1)\rangle_E$$

$$\times\langle M(0)[M(\tau_1),[M(\tau_1+\tau_2),M(\tau_1+\tau_2+\tau_3)]]\rangle_S\Bigg\}. \tag{6}$$

This is the statistical expression that was desired, which is valid in the parallel polarization case. It involves four-time correlation functions of the variable M, the component of the electric moment $\mathbf{M}$ in the field direction. It also includes a four-time correlation function of E and E_2, the total and probe electric fields, respectively. The average $\langle\ \rangle_S$ is an equilibrium average over the states of the field-free liquid sample and the average $\langle\ \rangle_E$ over different realizations of the incident electric fields. It can easily be shown that, although $M(\mathbf{r}_0)$ depends on the reference point $\mathbf{r}_0$, $S(\Omega_1,\Omega_2,\tau)$ does not. A convenient, though arbitrary, choice of $\mathbf{r}_0$ is in the middle of the experimental or simulation cell.

Equation (6) plays a central role in the statistical description of pump-probe absorption of the hydrated electron. Its counterpart in transient ir spectroscopy is given in Refs. [36, 38]; the latter paper refers to the arbitrary polarization case. The corresponding formula of conventional absorption spectroscopy is the well-known Gordon formula [41]. The pump-probe spectroscopy being a second-order spectroscopy, it involves four-time rather than two-time correlation functions; and the Fourier transform is replaced by a four-dimensional integral depending on the shape of the pulses. This is the price to pay for passing from the Kubo linear to nonlinear response theories.

B. Correlation functions

The following semiclassical model is employed in this work. (i) The aqueous solution is assimilated to a quantum-electronic system having an s-type ground state, three closely spaced p-type states $p=\{p_x,p_y,p_z\}$, and an allowed energy band containing n states $c=\{c_1,c_2,\ldots,c_n\}$ (Fig. 1). It is perturbed by stochastic solvent-solute interactions. The thermic bath, depending on the rotational-translational degrees of freedom, is semiclassical; water molecules are supposed to be rigid. (ii) The variable M is governed by the modified Heisenberg equation

$$\frac{dM}{dt}=\frac{i}{\hbar}[H,M]-\mathbf{\Gamma}M, \tag{7}$$

where H is an adiabatic Hamiltonian and $\mathbf{\Gamma}$ a Pauli matrix. This matrix expresses the population relaxation due to the

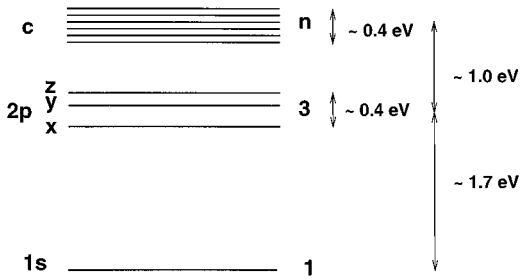

FIG. 1. Energy level diagram of e_{aq}^-. These levels are randomly fluctuating in time. The numbers of the first right-hand-side column refer to the electronic states involved.

coupling of the Born-Oppenheimer states [20,21]. (iii) The matrix elements of $H(t)$, $H_{ss}(t)$, $H_{pp}(t)$, $H_{cc}(t)$ are classical. The only nonvanishing elements of the electric moment matrix are M_{sp}, M_{ps}, M_{pc}, M_{cp}, and those of the relaxation matrix are Γ_{spsp}, Γ_{psps}, Γ_{pcpc}, Γ_{cpcp}. (iv) The pump and probe electric fields have a Gaussian profile of equal duration and random phases, independent of each other:

$$E_1(\mathbf{r},t)=\mathrm{Re}\{E_{10}\exp(-\gamma t'^2)\exp[i(\mathbf{k}_1\cdot\mathbf{r}-\Omega_1 t)]\times\exp[i\phi_1(t')]\}=\mathrm{Re}[\hat{E}_1(\mathbf{r},t)], \tag{8a}$$

$$E_2(\mathbf{r},t)=\mathrm{Re}\{E_{20}\exp(-\gamma t^2)\exp[i(\mathbf{k}_2\cdot\mathbf{r}-\Omega_2 t)]\times\exp[i\phi_2(t)]\}=\mathrm{Re}[\hat{E}_2(\mathbf{r},t)], \tag{8b}$$

where $t'=t+\tau$. The duration of the incident pulse is $\tau_E\sim 1/\sqrt{\gamma}$.

Although models of this type are of current use in nonlinear spectroscopy, their application to the problem of hydrated electron deserves some comments. (i) Introducing a thermic bath renders the study of the ground-state heating or cooling dynamics uneasy. However, this mechanism does not seem to provide the dominant explanation for the observed spectroscopy [27] and is disregarded. (ii) The energy gap between different electronic states is continuously changing due to solvent motions; there results a multiexponential decay of excited populations. However, in the simplest theory, a single rate constant Γ may suffice. The model can be improved at this point, if the price of this effort is accepted.

The calculation of the electric moment correlation functions can now be undertaken; compare with [36,37]. Molecular rotations being slow at the 100-fs time scale, they are neglected altogether. As far the operation $\langle\ \rangle_S$ is concerned, it implies averaging over the quantum states s,p,c of the hydrated electron as well as that over the stochastic process $H_{ss}(t)$, $H_{pp}(t)$, $H_{cc}(t)$. Then, designating the latter by $\langle\ \rangle$ and noting that only the ground electronic state is thermally populated, results in

$$\langle M(0)M(t_1)M(t_2)M(t_3)\rangle_S=\sum_p\langle M_{sp}(0)M_{ps}(t_1)M_{sp}(t_2)M_{ps}(t_3)\rangle+\sum_{pc}\langle M_{sp}(0)M_{pc}(t_1)M_{cp}(t_2)M_{ps}(t_3)\rangle. \tag{9}$$

The first right-hand-side term of Eq. (9) describes the ground-state bleach, including the contribution due to the $p\rightarrow s$ stimulated emission. Similarly, its second right-hand-side term reproduces the induced $p\rightarrow c$ absorption.

The matrix elements $M_{ij}(t)$ of the electric moment operator are calculated by solving Eq. (4) under the assumptions of the present model. One finds that $M_{ii}(t)=0$ and $M_{ij}(t)=M_{ij}(0)\exp[i\int_0^t dt'\,\omega_{ij}(t')-\Gamma_{ijij}t]$, where $\hbar\omega_{ij}(t)=E_i(t)-E_j(t)$. Other steps are as follows. (i) The $s\leftrightarrow p$ component of the correlation function is determined by using the cumulant expansion theorem. The transition moments M_{sp} are all supposed to be equal to M, such that $M^4=\frac{1}{3}\Sigma_p\langle M_{sp}^4\rangle$. (ii) The calculation of the $p\rightarrow c$ component of Eq. (9) requires some knowledge of the density of electronic states $g(\omega)$ inside the energy band. It may reasonably be assumed to have a Gaussian form:

$$g(\omega)=\frac{n}{\sqrt{\pi}\Delta\omega}\exp\left(-\frac{(\omega-\omega_1)^2}{\Delta\omega^2}\right), \tag{10}$$

where $\hbar\omega_1$ indicates its center and $\hbar\Delta\omega$ its width. The transition moments M_{pc} are all supposed to be equal to M', such that $M^2M'^2=(1/3n)\Sigma_{pc}\langle M_{sp}^2M_{pc}^2\rangle$. (iii) The final correlation function contains contributions proportional to

$$C_{\pm}(\tau_1,\tau_2,\tau_3)=\exp(-\Gamma(\tau_1+2\tau_2+3\tau_3))\times\exp[-\tfrac{1}{2}\beta\tau_1^2-\tfrac{1}{2}\beta\tau_3^2\pm\tau_1\tau_3\beta(\tau_1+\tau_2)], \tag{11a}$$

$$D_{\pm}(\tau_1,\tau_2,\tau_3)=\exp[-\Gamma(\tau_1+2\tau_2+3\tau_3)]\times\exp[-\tfrac{1}{2}\beta'\tau_1^2-\tfrac{1}{2}\beta\tau_3^2\pm\tau_1\tau_3\beta(\tau_1+\tau_2)], \tag{11b}$$

where $\beta(\tau)=\langle\omega(0)\omega(\tau)\rangle_c$, $\beta=\beta(0)$, $\beta'=\beta+\Delta\omega^2/2$, $\omega(\tau)$ is the solvent-induced frequency shift, and the symbol $\langle\ \rangle_c$ denotes a cumulant. The first factor in Eqs. (11a) and (11b) describes the population relaxation, and the second the solvent relaxation. These formulas only apply if the electronic dephasing time $\tau_d\sim 1/\sqrt{\beta}$ is short with respect to the correlation time τ_Ω of $\beta(\tau)$; electronic motions, in fact, are fast compared to nuclear motions.

The calculation of the electric-field correlation function $\langle\dot{E}_2(\mathbf{r},t)E(\mathbf{r},t-\tau_3)E(\mathbf{r},t-\tau_3-\tau_2)E(\mathbf{r},t-\tau_3-\tau_2-\tau_1)\rangle_E$ is similar to that described in Ref. [36]; it will only be sketched in what follows. (i) The time derivative $\dot{E}_2(\mathbf{r},t)$ of the probe is calculated by deriving only the rapidly varying factor $\exp(i\Omega_2 t)$. (ii) The incident fields are decomposed into individual exponentials. A large number of terms result. However, if the contributions of the order of E_2^4 are neglected, which is a coherent assumption, only those having the form $\langle\hat{E}_2^*(\mathbf{r},t_1)\hat{E}_2(\mathbf{r},t_2)\hat{E}_1^*(\mathbf{r},t_3)\hat{E}_1(\mathbf{r},t_4)\rangle_E$ survive after integration over $\mathbf{r}$. (iii) The averaging over the random phases $\phi_1(t)$, $\phi_2(t)$ is accomplished by applying the cumulant expansion theorem, and by supposing these processes to be Gaussian and slowly modulated: $\dot{\phi}_1\tau_\phi\gg 1$, $\dot{\phi}_2\tau_\phi\gg 1$, where τ_ϕ is the phase correlation time. The final correlation functions then contain terms like

$$E_{10}^2E_{20}^2\exp[i\Omega_2(t_1-t_2)+i\Omega_1(t_3-t_4)]\exp[-\gamma(t_1^2+t_2^2+t_3'^2+t_4'^2)]\exp[-\tfrac{1}{2}(t_1-t_2)^2\phi-\tfrac{1}{2}(t_3-t_4)^2\phi], \tag{12}$$

where t_1, t_2, t_3, and t_4 are different combinations of times t, $t-\tau_3$, $t-\tau_3-\tau_2$, $t-\tau_3-\tau_2-\tau_1$, and $\phi=\langle\dot{\phi}_1^2\rangle=\langle\dot{\phi}_2^2\rangle$. Other noise models, such as the phase diffusion, telegraph or Burshtein model [42] could have been used, but the existing experimental data are insufficient to justify this effort.

C. Signal $S(\Omega_1,\Omega_2,\tau)$

There still remains to perform the four-dimensional integrations over the variables t, τ_1, τ_2, and τ_3 in Eq. (6). The methods employed, as well as the results, depend heavily on characteristic times of the problem. In what follows, the integrals are evaluated in the limit $\tau_d \ll \tau_\Omega \ll \tau_E$, τ_p if the light is coherent and in the limit $\tau_d \ll \tau_\Omega$, $\tau_\phi \ll \tau_E$, τ_p if it is incoherent; τ_p is the population relaxation time. The computer simulations described in the next section confirm the existence of the above constraints. The correlation function $\beta(\tau)=\langle\omega(0)\omega(\tau)\rangle_c$ is written in the form of a single Heaviside step function depending on a time τ_Ω. This makes precise analytical calculations practicable, although they still are highly nontrivial; no factorization of the integrands into smaller units can be achieved. A large part of the overall computational effort is concentrated in this part of the work.

The shape of the signal $S(\Omega_1,\Omega_2,\tau)$ is different for coherent and incoherent incident fields; one recalls that $\tau_\phi \to \infty$ in the former case, whereas $\tau_\phi \lesssim \tau_\Omega$ in the latter. Let then $S_{s\leftrightarrow p}(\Omega_1,\Omega_2,\tau)$ designate the contribution to $S(\Omega_1,\Omega_2,\tau)$ associated with the transitions $s\leftrightarrow p$, $S_{p\to c}(\Omega_1,\Omega_2,\tau)$ that due to transitions $p\to c$ and $S(\Omega_1,\Omega_2,\tau)=-S_{s\leftrightarrow p}(\Omega_1,\Omega_2,\tau)+S_{p\to c}(\Omega_1,\Omega_2,\tau)$. For coherent incident fields and for $\tau_d \ll \tau_\Omega \ll \tau_E$, τ_p, one finds

$$S_{s\leftrightarrow p}(\Omega_1,\Omega_2,\tau)\left[3N\,\frac{\Omega_2}{\hbar^3}\,M^4E_{10}^2E_{20}^2\,\frac{\pi}{\gamma}\,\frac{\pi}{\beta}\right]^{-1}=\left(\left\{1+\mathrm{erf}\left[\sqrt{\gamma}\left(\tau-\frac{\Gamma}{\gamma}\right)\right]\right\}\exp\left[-2\Gamma\left(\tau-\frac{\Gamma}{2\gamma}\right)\right]\exp\left[-\frac{1}{2\beta}\,(\Delta_1^2+\Delta_2^2)\right]\right.$$
$$+\frac{2}{\sqrt{\pi}}\exp(-\gamma\tau^2)\exp(\Gamma^2/\gamma)\exp\left(-\frac{\Delta_1^2}{\beta}\right)\sqrt{\gamma}W\left(\frac{\Gamma}{\gamma},\Delta,\gamma\right)$$
$$\left.+\frac{2\sqrt{2}}{\pi}\,\sqrt{\gamma}\tau_\Omega\sqrt{\beta}\tau_\Omega\exp(-\gamma\tau^2)\,\frac{\sin(\Delta\tau_\Omega)}{\Delta\tau_\Omega}\,\exp\left(-\frac{\Delta_2^2}{2\beta}\right)\right), \tag{13a}$$

$$S_{p\to c}(\Omega_1,\Omega_2,\tau)\left[\frac{3}{2}\,N\,\frac{\Omega_2}{\hbar^3}\,nM^2M'^2E_{10}^2E_{20}^2\,\frac{\pi}{\gamma}\,\frac{\pi}{\sqrt{\beta((\Delta\omega)^2/2+\beta)}}\right]^{-1}=\left\{1+\mathrm{erf}\left[\sqrt{\gamma}\left(\tau-\frac{\Gamma}{\gamma}\right)\right]\right\}\exp\left[-2\Gamma\left(\tau-\frac{\Gamma}{2\gamma}\right)\right]$$
$$\times\exp\left(-\frac{\Delta_1^2}{2\beta}\right)\exp\left(-\frac{\Delta_2'^2}{(\Delta\omega)^2+2\beta}\right), \tag{13b}$$

$$W(t,\delta,\gamma)=\int_0^\infty d\tau\,\cos\delta\tau\,\exp(-\gamma(\tau+t)^2), \tag{13c}$$

where N is the number of solvated electrons, $\Delta_1=\Omega_1-\omega_0$, $\Delta_2=\Omega_2-\omega_0$, $\Delta=\Omega_1-\Omega_2$, $\Delta_2'=\Omega_2-\omega_0'$, $\hbar\omega_0=\hbar(\langle\omega_{px\to s}\rangle+\langle\omega_{py\to s}\rangle+\langle\omega_{pz\to s}\rangle)/3$, $\hbar\omega_0'=\hbar(\omega_1-\omega_0)$, and $1/2\Gamma=\tau_p$. All Γ_{ijij} are given the same value Γ.

If the incident electric fields are incoherent, the theory takes another form. Introducing the conditions $\tau_d \ll \tau_\Omega$, $\tau_\phi \ll \tau_E$, τ_p, leads to the following expressions for the components $S_{s\leftrightarrow p}(\Omega_1,\Omega_2,\tau)$ and $S_{p\to c}(\Omega_1,\Omega_2,\tau)$ of $S(\Omega_1,\Omega_2,\tau)$:

$$S_{s\leftrightarrow p}(\Omega_1,\Omega_2,\tau)\left[3N\,\frac{\Omega_2}{\hbar^3}\,M^4E_{10}^2E_{20}^2\,\frac{\pi}{\gamma}\,\frac{\pi}{\beta}\right]^{-1}=\left(\left\{1+\mathrm{erf}\left[\sqrt{\gamma}\left(\tau-\frac{\Gamma}{\gamma}\right)\right]\right\}\exp\left[-2\Gamma\left(\tau-\frac{\Gamma}{2\gamma}\right)\right]\exp\left[-\frac{1}{2\beta}\,(\Delta_1^2+\Delta_2^2)\right]\right.$$
$$\left.+\frac{2\sqrt{2}}{\pi}\,\sqrt{\gamma}\tau_\Omega\sqrt{\beta}\tau_\Omega\exp(-\gamma\tau^2)\,\frac{1}{\tau_\Omega}\,U(\tau_\Omega,\Delta,\phi)\exp\left(-\frac{\Delta_2^2}{2\beta}\right)\right), \tag{14a}$$

$$S_{p\to c}(\Omega_1,\Omega_2,\tau)\left[\frac{3}{2}\,N\,\frac{\Omega_2}{\hbar^3}\,nM^2M'^2E_{10}^2E_{20}^2\,\frac{\pi}{\gamma}\,\frac{\pi}{\sqrt{\beta((\Delta\omega)^2/2+\beta)}}\right]^{-1}=\left\{1+\mathrm{erf}\left[\sqrt{\gamma}\left(\tau-\frac{\Gamma}{\gamma}\right)\right]\right\}\exp\left[-2\Gamma\left(\tau-\frac{\Gamma}{2\gamma}\right)\right]$$
$$\times\exp\left(-\frac{\Delta_1^2}{2\beta}\right)\exp\left(-\frac{\Delta_2'^2}{(\Delta\omega)^2+2\beta}\right), \tag{14b}$$

$$U(t,\delta,\gamma)=\int_0^t d\tau\,\cos\delta\tau\,\exp(-\gamma\tau^2). \tag{14c}$$

The symbols have the same meaning as earlier. The main difference between Eqs. (13a)–(13c) and Eqs. (14a)–(14c) is the presence of a coherent artifact in the former and its absence in the latter, if $\Omega_1 \sim \Omega_2$ and $\tau \sim \tau_E$. One recalls that the term ''coherent artifact'' designates any spectral feature resulting from the phase relations between the pump and probe fields.

The above formulas for the band shape constitute the end result of the statistical theory. It remains to calculate the parameters entering into them by computer simulation. If the absolute value of spectral intensities is not required, one has to determine the quantities n, ω_0, ω_0', $\Delta\omega$, $\beta = \langle \omega(0)^2 \rangle_c$, τ_p, τ_Ω, τ_d, and M'^2/M^2. They have all a precise statistical meaning and will be studied in the next section.

III. COMPUTER SIMULATION

A. Methodological details

The purpose of this section is to outline the key features of the mixed quantum-classical molecular-dynamics simulation used to compute the various statistical quantities defined in the preceding section. The method employed is an adiabatic simulation method in which the electron is constrained to a specific quantum state. The rate of nonadiabatic transitions is calculated by employing the Fermi golden rule. The solvent evolves classically in these calculations. A careful discussion of technical details is given in Ref. [23].

It is important to note that, in the theory of Sec. II, as in the linear response theory, the final results are expressed in terms of quantities averaged over the nonperturbed states of the system in thermal equilibrium. Field-induced changes of molecular dynamics, both in the ground and excited states, are accounted for by passing from the two- to the four-time correlation functions in Eq. (6). The third right-hand-side term of Eq. (13a), or the second right-hand-side term of Eq. (14a), express this effect. The window and doorway operators, well known in the literature, have a similar origin [33].

The system considered here consists of 255 rigid, polarizable water molecules and of an extra electron. (i) The solvent is represented by the model of Sprik and Klein [43,44]. In this model, the solvent molecules interact with each other via the Lennard-Jones, Coulomb, and polarization forces, generating a potential V_{ss}. A positive charge $q_H = 0.4428$ e.u. is placed on each hydrogen atom, and a negative charge $q_M = -0.2214$ e.u. on each vertex of a tetrahedron, with its center slightly shifted away from the oxygen atom in the HOH plane. The dipole moment of free H_2O is correctly described in this way. In order to account for electronic polarization of the solvent, additional fluctuating charges q_i are introduced on the tetrahedral sites: they are computed iteratively as described below. Polarization instability is avoided by using Gaussian polarization charges instead of mere point charges. (ii) The electron is pictured by the so-called primitive model of Romero and Jonah [16], and Sprik [45]. e_{aq}^- is coupled to the solvent through electrostatic and polarization forces, deriving from the pseudopotential

$$V_{es} = \sum_{i=1}^{2} \mathrm{e}(\mathrm{q}_H) \frac{\mathrm{erf}(\alpha_H |\mathbf{r} - \mathbf{R}_{H_i}|)}{|\mathbf{r} - \mathbf{R}_{H_i}|} - \sum_{i=1}^{4} e(q_M + q_i) \frac{\mathrm{erf}(\alpha_M |\mathbf{r} - \mathbf{R}_{M_i}|)}{|\mathbf{r} - \mathbf{R}_{M_i}|}, \quad (15)$$

where $\mathbf{R}_{H_i}$, $\mathbf{R}_{M_i}$ denote the positions of the hydrogens and of the tetrahedron vertices in a given water molecule and $\mathbf{r}$ is the electron coordinate. All interactions are smoothly damped at short distances; this effect is described by damping parameters α_H and α_M.

The excess electron being coupled to the solvent, the electronic wave functions Ψ_n depend on the coordinates $\mathbf{r}$ and $\mathbf{S} = \{\mathbf{R}_H, \mathbf{R}_{M_i}\}$. It is then convenient to expand them into a basic set of floating spherical Gaussians $g_i(\mathbf{r})$:

$$\Psi_n(\mathbf{r}, \mathbf{S}) = \sum_{i=1}^{N} a_{ni}(\mathbf{S}) g_i(\mathbf{r}). \quad (16)$$

The rationale behind this proposal is as follows. As a hydrated electron is freely diffusing through the liquid, it cannot be described successfully in terms of atomic orbitals fixed on individual water molecules. Floating orbitals, i.e., orbitals detached from the parent nuclei, are thus preferable. They are placed on vertices of a regular polyhedron. The whole entity diffuses through the solvent; it fluctuates in shape and size due to an instantaneous change of the weight of individual orbitals. The calculations are realized by introducing one s-type Gaussian at the origin of the polyhedron, four s/p Gaussians placed on the vertices of a tetrahedron, 12 $s/p/d$ Gaussians placed on the vertices of an icosahedron, etc. The usual advantage of Gaussian basis sets, i.e., the rapid analytical evaluation of integrals and matrix elements is exploited here. Since this basis is local, its origin must be adjusted continuously to ensure a proper representation of the solute electronic wave function at a given time.

The molecular-dynamics simulations are carried out in the following way. (i) The energies and expansion coefficients of the electronic wave functions $\Psi_n(\mathbf{r}, \mathbf{S})$ are calculated for a fixed nuclear configuration and for a given initial set of polarization charges. (ii) The computed electronic densities, added to the initial polarization charges, permit us to define the new ones; the cycle is repeated until the convergence is attained. (iii) Once the polarization is optimized, the e_{aq}^--solvent forces are determined via the Hellmann-Feynman theorem; they are always computed for the same quantum state. (iv) A new solvent configuration is generated by a classical molecular-dynamics simulation. The forces entering into equations of motion are the solvent-solvent plus the e_{aq}^--solvent forces just described.

When studying the excitation of e_{aq}^- from one accessible state to another, the polarization must be optimized independently for each individual state. This is computationally much more demanding than a simpler variant, where all states have the same polarization charges. The effect is by no means negligible: it was shown, for example, that computing

the stationary absorption spectrum of the hydrated electron with the full optimization for each state shifts the band maximum by 0.3 eV, and locates it properly to 1.7 eV.

All simulations were performed at 298 K in a cubic simulation cell of 19.96 Å length. The equations of motions were integrated using the leapfrog quaternion algorithm with a time step of 0.5 fs. The long-range electrostatic potentials and corresponding forces were evaluated with the Ewald summation technique employing periodic boundary conditions and a uniform background of charge. As mentioned earlier, the mobility of the electron is accounted for by moving adiabatically the center of the bunch of Gaussian orbitals in the course of the simulation. At each time step the wave function $\Psi_0(\mathbf{r},\mathbf{S})$ is used to calculate the center $\mathbf{r}_0 = \langle \Psi_0(\mathbf{r},\mathbf{S})|\mathbf{r}|\Psi_0(\mathbf{r},\mathbf{S})\rangle$ of the electronic cloud in its ground state. The vector $\mathbf{r}_0$ is then identified with the origin of the basis set for the next molecular-dynamics step. An *a posteriori* justification of this procedure is the good conservation of the total energy, which is of the order of 0.1% for a 5-ps trajectory. The fact that the temperature fluctuations are small, $\Delta T \sim 4$ K, is another test of the quality of the present simulation.

B. Calculation of parameters

Once the techniques of calculation have been described, the evaluation of the energy-band parameters n, $\Delta\omega$, of the equilibrium properties ω_0, ω_0', β, M^4, M'^2M^2 and of the dynamical properties τ_Ω, τ_p may be envisaged. The parameters τ_E and τ_ϕ, deducible from the spectral width of the incident pulses, do not need to be considered here [46]. The following points merit attention. (i) The frequencies ω_0, ω_0', and β are calculated by averaging the energies, energy differences, and their squares. This averaging is over the ground-state trajectories, as required. The resulting values are in excellent agreement with spectroscopic data of Ref. [47]. Introducing polarization thus improves the quality of the results considerably. (ii) The transition moments are computed by a direct application of statistical definitions. There is no difficulty for $M^4 = (\frac{1}{3})\Sigma_p \langle M_{sp}^4 \rangle$. On the contrary, the accuracy of $M'^2M^2 = (1/3n)\Sigma_{pc}\langle M_{sp}^2 M_{pc}^2\rangle$ is limited, due to the reduced size of the basic set of Gaussian orbitals. It was found that, in the spectral region under investigation, five c states are detached from the rest and that the corresponding transition moments are comparatively large; the values of n and $\Delta\omega$ refer to this group of states. The delocalized states, if any, cannot contribute very much to the spectral intensity: the overlap between the localized s, p, and delocalized c-type wave functions is necessarily small.

The parameter τ_Ω is extracted from the normalized frequency shift correlation function $\beta(t)/\beta(0)$. This function, determined from an extensive ground-state trajectory, may be represented by an expression of the form

$$\beta(t)/\beta(0) = c_1 \exp\left(-\frac{t^2}{\tau_{\Omega_1}^2}\right) + c_2 \exp\left(-\frac{t}{\tau_{\Omega_2}}\right), \quad (17)$$

where $c_1 = 0.465$, $c_2 = 0.535$, $\tau_{\Omega_1} = 17$ fs, and $\tau_{\Omega_2} = 130$ fs. The initial Gaussian decay occurs on a very short time scale, typical of the inertial component of the librational motions of H_2O. Equation (17) was used to calculate $\langle M(0)M(t_1)M(t_2)M(t_3)\rangle s$. The results are illustrated in Fig. 2. Comparing Figs. 2(a) and 2(c) with 2(b) and 2(d), one notices that the contribution of inertial motions to these functions is particularly important. This unexpected observation can be understood in the following way. If $\beta(t)$ contains two components, $\beta(t) = \beta_1(t) + \beta_2(t)$, the electronic correlation functions $C_\pm(\tau_1,\tau_2,\tau_3)$ and $D_\pm(\tau_1,\tau_2,\tau_3)$ of Eqs. (11a) and (11b) all factorize:

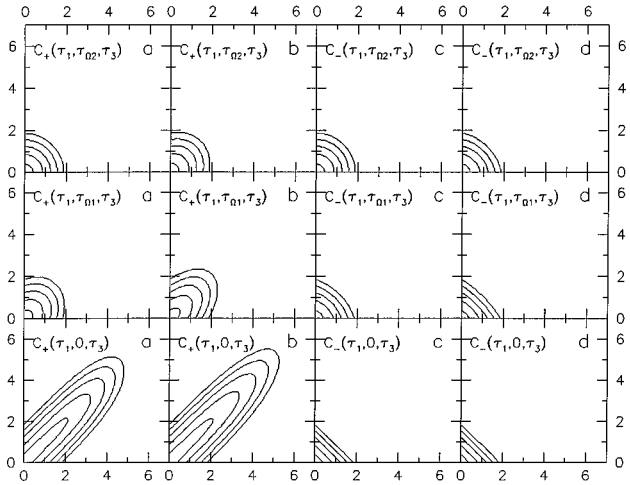

FIG. 2. The functions $C\pm(\tau_1,\tau_2,\tau_3)$ calculated either with the monoexponential correlation function $\beta(t) = \beta\exp(-t^2/\tau_{\Omega1}^2)$ (a,c) or with the biexponential correlation function $\beta(t) = \beta[0.465\ \exp(-t^2/\tau_{\Omega1}^2) + 0.535\ \exp(-t/\tau_{\Omega2})]$ (b,d) where $\tau_{\Omega1} = 17$ fs, $\tau_{\Omega2} = 130$ fs, and $\tau_2 = 0$, $\tau_{\Omega1}$, and $\tau_{\Omega2}$. The figures represent the curves of equal height of $C\pm(\tau_1,\tau_2,\tau_3)$ corresponding to the values of 0.98, 0.90, 0.80, 0.70, and 0.60, respectively. Similar objects occur in two-dimensional NMR.

$$C_\pm(\tau_1,\tau_2,\tau_3) = \exp[-\Gamma(\tau_1 + 2\tau_2 + 3\tau_3)] \times \exp[-\tfrac{1}{2}\beta_1\tau_1^2 - \tfrac{1}{2}\beta_1\tau_3^2 \pm \tau_1\tau_3\beta_1(\tau_1+\tau_2)] \times \exp[-\tfrac{1}{2}\beta_2\tau_1^2 - \tfrac{1}{2}\beta_2\tau_3^2 \pm \tau_1\tau_3\beta_2(\tau_1+\tau_2)],$$

$$D_\pm(\tau_1,\tau_2,\tau_3) = \exp[-\Gamma(\tau_1 + 2\tau_2 + 3\tau_3)] \times \exp[-\tfrac{1}{2}\beta_1'\tau_1^2 - \tfrac{1}{2}\beta_1\tau_3^2 \pm \tau_1\tau_3\beta_1(\tau_1+\tau_2)] \times \exp[-\tfrac{1}{2}\beta_2'\tau_1^2 - \tfrac{1}{2}\beta_2\tau_3^2 \pm \tau_1\tau_3\beta_2(\tau_1+\tau_2)],$$

where $\beta_1 = \beta_1(0)$, $\beta_2 = \beta_2(0)$, $\beta_1' = \beta_1 + \Delta\omega^2/4$, and $\beta_2' = \beta_2 + \Delta\omega^2/4$. If $\sqrt{\beta_1}\tau_{\Omega1} \gg 1$, the fast motions make the second right-hand-side factor of $C_\pm, D_\pm$, and these functions themselves, very small for $\tau_1, \tau_3 \gg \tau_{\Omega1}$, $\forall\,\tau_2$. Spectral manifestations of slow motions, expressed by the third right-hand-side factor of $C_\pm, D_\pm$ cannot be very large in these conditions. The argument holds true even if $c_1 \sim c_2$. One concludes that most of the spectral evolution of solvation of the electron is achieved by the fast, 20-fs inertial response of the solvent; nevertheless, some spectral dynamics occur on

TABLE I. Parameters defining the signal $S(\Omega_1,\Omega_2,\tau)$. Energies are expressed in eV and times in femtoseconds; the quantities n and M'^2/M^2 are dimensionless. They are all computed by simulation, except the field parameters τ_ϕ and τ_E, which are extracted from Refs. [9,46].

$\hbar\omega_0$	1.74	τ_d	1
$\hbar\omega_0'$	1.05	τ_Ω	17
$\hbar\sqrt{\beta}$	0.285	τ_ϕ	14
$\hbar\Delta\omega$	0.190	τ_p	910
n	5	τ_E	130
M'^2/M^2	1.3		

the time scale of the slow solvation component [9]. Attributing to $\beta(t)$ the form of a step function of length $\tau_\Omega \sim \tau_{\Omega 1}$ is thus an acceptable procedure.

The calculation of the parameter $\tau_p = \frac{1}{2}\Gamma$ is more difficult. Since the s,p,c states introduced for the description of the hydrated electron are by definition the Born-Oppenheimer states, i.e., the electronic states at a fixed nuclear positions, the transitions between them are due to the nuclear kinetic energy. The golden rule then states that in a system composed of nuclei of masses M_α and having the Born-Oppenheimer states $\Psi_{\beta\gamma} = \phi_\beta \chi_{\beta\gamma}$ of energies $E_{\beta\gamma}$ the population relaxation times are given by $\tau_{i\to f}^{-1} = \int_{-\infty}^{\infty} dt \langle V_{if}(0) V_{fi}(t)\rangle$, where

$$V_{if} = \frac{1}{\hbar} \sum_l \frac{1}{2M_l} [2\langle \phi_i | \mathbf{P}_l | \phi_f \rangle \mathbf{P}_l + \langle \phi_i | \mathbf{P}_l^2 | \phi_f \rangle] \quad (18)$$

and $\mathbf{P}_\alpha$ is the momentum of the nucleus α; the summation over l extends over all nuclei of the system [21]. In the present work, $\tau_{i\to f}$ was calculated in the semiclassical approximation. The approximation consists in (i) neglecting the second right-hand-side term in Eq. (18) and (ii) assimilating the symmetrized form of $\langle V_{if}(0) V_{fi}(t)\rangle$ to a classical correlation function. Note that the nuclei are treated as classical interaction sites, and do not need to be represented by frozen quantum Gaussians. This statement conforms to a general rule of statistical mechanics: classical mechanics may be used whenever $\hbar\omega \ll k_B T$, where $\hbar\omega$ is a representative energy of the process under investigation. Rotational-translational motions of H_2O molecules in water fulfill this condition at room temperature; vibrational motions are absent in the present model where water molecules are considered as rigid. For a discussion of semiclassical approximations of the golden rule in molecular liquids, see Ref. [48].

The value of parameters obtained in this way are collected in Table I. They confirm the existence of inequalities $\tau_d \ll \tau_\Omega \ll \tau_E, \tau_p$, and $\tau_d \ll \tau_\Omega$, $\tau_\phi \ll \tau_E$, τ_p postulated in Sec. II. The value of 910 fs found for τ_p is somewhat larger than that published earlier with a poorer statistics [23]. The values reported in the literature are spread between 100 fs and 1 ps [21,24,26,29]. In fact, the computation of nonadiabatic transition rates is sensitive to the choice of the electron-water pseudopotential, to the quality of its statistics, and to whether the H_2O molecule is considered rigid or flexible; the results are not yet entirely conclusive on this point. All other parameters of Table I are similar to those published elsewhere; it is interesting to compare τ_p with recent model calculations

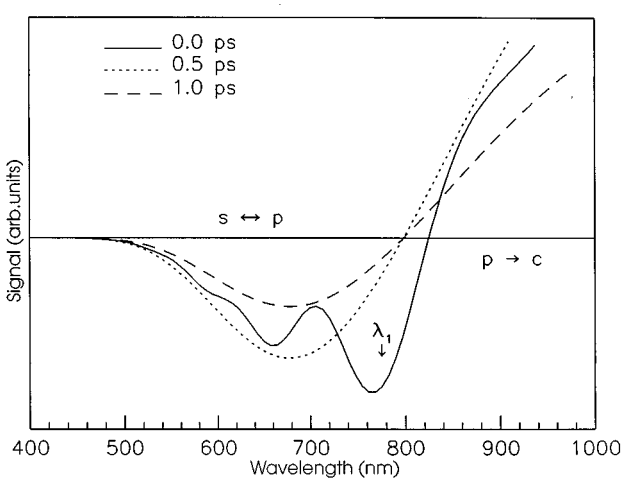

FIG. 3. Theoretical frequency-resolved spectra calculated with $\lambda_1 = 780$ nm and $\tau = 0$, 0.5, and 1.0 ps. Incident light is incoherent. The nonthermic $s \leftrightarrow p$ subband is centered at the pump wavelength λ_1. Its intensity is very sensitive to the value of τ_Ω.

[49]. The signals $S(\Omega_1,\Omega_2,\tau)$ given by Eqs. (13a)–(13c) and (14a)–(14c) may now be evaluated and compared with those measured experimentally. The results reached in this way will be discussed in the next section.

IV. RESULTS AND DISCUSSION

A. Results

This theory provides the following physical picture of the transient absorption of the hydrated electron. To simplify the discussion, the incident light is supposed to be incoherent; spectral effects produced by coherent radiation will be only briefly mentioned at the end. The analysis then goes as follows. The pump pulse, exciting coherently a set of solvent configurations, creates the initial wave packet. The latter decays toward the equilibrium with time scales of the order of τ_Ω, τ_p. The solvent relaxation is described by the frequency shift correlation function $\beta(t)$; $\beta(t)/\beta(0)$ is just the well-known response function $S(t)$, currently employed to analyze time-resolved fluorescence [50]. In turn, the population relaxation is accounted for by the element Γ of the Pauli relaxation matrix. Two groups of solvent configurations may then be distinguished. Those remaining in the window produce a comparatively narrow band centered on the pump frequency Ω_1; generated by the absorption of the initial wave packet and thus having a nonthermal origin, it will be termed a ''coherent spike'' hereafter. From the other side, the solvent configurations, having undergone the thermalization process, escape the initial spectral window and generate a ''thermic'' band. The main features of the pump-probe absorption of the hydrated electron are due to the coexistence of these two sorts of bands.

Starting from the above considerations, the frequency-resolved spectra may now be analyzed; compare with Eqs. (14a)–(14c) and Fig. 3. (i) The transient signal contains a component $S_{s\leftrightarrow p}(\Omega_1,\Omega_2,\tau)$ and a component $S_{p\to c}(\Omega_1,\Omega_2,\tau)$. The former appears as a bleach, and the latter as an absorption. (ii) The bleach component $S_{s\leftrightarrow p}(\Omega_1,\Omega_2,\tau)$ is composite. It contains a broad thermic

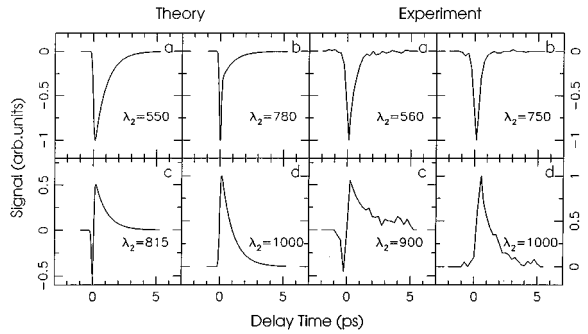

FIG. 4. Theoretical and experimental time-resolved spectra of e^--H_2O, calculated with $\lambda_1=780$ nm and $\lambda_2=550$, 780, 820, and 1000 nm. Except for small wavelength shifts, the agreement between theory and experiment is satisfactory.

sub-band of half-width $\Delta\omega_{1/2}\sim\sqrt{\beta}$, comparable to that of the conventional absorption band. This subband is given by the first right-hand-side term of Eq. (14a). Superposed on it is the coherent spike, located at the pump frequency Ω_1 and described by the function $(1/\tau_\Omega)U(\tau_\Omega,\Delta,\phi)$ of Eqs. (14a) and (14c). It displays diffractionlike characteristics if $\tau_\Omega\sqrt{\phi}\ll 1$; they disappear for time delays τ such that $\sqrt{\gamma}\tau \gg 1$. (iii) The induced absorption component $S_{p\to c}(\Omega_1,\Omega_2,\tau)$, given by Eq. (14b), contains only a thermic subband if the width $\Delta\omega$ of the allowed energy band is comparable to $\sqrt{\beta}$; this is supposed to be the case here. Theoretical frequency-resolved spectra of e^-_{aq} are given for three delay times τ. Unfortunately, no experimental data are as yet available. This is due to the difficulty in measuring relative intensities at different wavelengths.

The analysis of time-resolved spectra goes as follows: compare with Eqs. (14a)–(14c) and Figs. 4(a)–4(d). (i) The signal amplitude may be positive or negative, depending on the probe frequency Ω_2. (ii) The characteristics of time-resolved spectra are dominated by the fact that the buildup and decay of the thermic band and of the coherent spike, respectively, are very different. The corresponding transients $T_t(\tau)$ and $T_{cs}(\tau)$, normalized to unity, are

$$T_t(\tau)=C\left\{1+\mathrm{erf}\left[\sqrt{\gamma}\left(\tau-\frac{\Gamma}{\gamma}\right)\right]\right\}\exp\left[-2\Gamma\left(\tau-\frac{\Gamma}{2\gamma}\right)\right], \tag{19a}$$

$$T_{cs}(\tau)=\exp(-\gamma\tau^2), \tag{19b}$$

where C is a normalization constant. Thus, if Ω_2 is chosen far from Ω_1 where the thermic component dominates, the τ dependence of the signal is that of Eq. (19a); its temporal half-width is of the order of $\tau_p\sim\frac{1}{2}\Gamma$ [Figs. 4(a) and 4(d)]. If, on the contrary, Ω_2 is comparable to Ω_1 and the coherent spike dominates, the signal shape is described by Eq. (19b); the temporal half-width is then of the order of $\tau_E\sim 1/\sqrt{\gamma}$ [Fig. 4(b)]. Finally, in the intermediate regime, the competition of these subbands generates a nonmonotonic behavior [Fig. 4(c)]. (iii) The interplay between the thermic band and the coherent spike also dominates the isotope effect. As seen in Eq. (19a), the time evolution of a thermic transient depends on the nonadiabatic rate constant Γ. As Γ is isotope dependent, so is the corresponding transient. On the contrary,

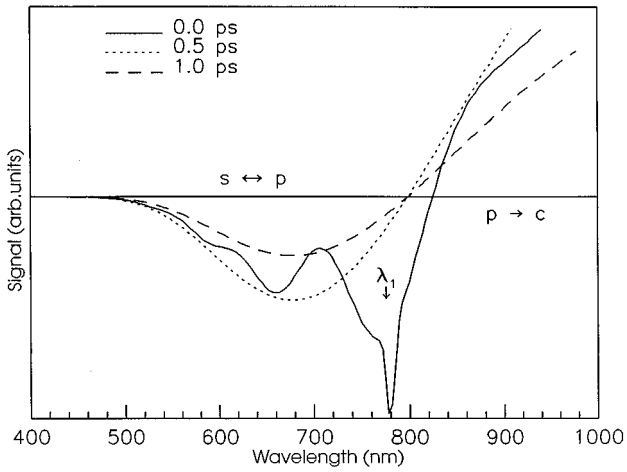

FIG. 5. Theoretical frequency-resolved spectra of e^--H_2O, calculated with $\tau=0$, 0.5, and 1.0 ps. Incident light is coherent. The presence of an artifact at the pump wavelength is characteristic of these spectra.

the time evolution of the coherent spike is just that of the pump pulse and is free of any isotope effect; compare with Eq. (19b). The theory thus predicts an isotope effect in the wings of the absorption band, but not in the vicinity of the pump frequency. The published simulation work on the isotope effect on Γ is still controversial [21,51]; if it is small, as claimed in Ref. [51], spectral changes will be small, even in the wings. Although no fitting procedure was employed to fix the parameters, the agreement between theory and experiment [8,9] is, except for minor wavelength shifts, surprisingly good.

The above analysis may be completed by briefly describing spectral effects of coherent light. The frequency-resolved spectra remain similar to those just described, but an artifact appears, as a bleach, around the pump frequency Ω_1 for time delays $\tau\lesssim 1/\sqrt{\gamma}$. Its shape $\Delta S(\Omega_1,\Omega_2,\tau)$ is given by

$$\Delta S(\Omega_1,\Omega_2,\tau)\left[3N\frac{\Omega_2}{\hbar^3}M^4E_{10}^2E_{20}^2\frac{\pi}{\gamma}\frac{\pi}{\beta}\right]^{-1}$$
$$=-\frac{2}{\sqrt{\pi}}\exp(-\gamma\tau^2)\exp\left(\frac{\Gamma^2}{\gamma}\right)$$
$$\times\exp\left(-\frac{\Delta_1^2}{\beta}\right)\sqrt{\gamma}W\left(\frac{\Gamma}{\gamma},\Delta,\gamma\right); \tag{20}$$

compare with Eqs. (13a)–(13c). If, as in the present case, $\Gamma/\sqrt{\gamma}\ll 1$, the ratio between the peak intensities of the artifact and of the coherent spike is of the order of $(\sqrt{\gamma}\tau_\Omega\sqrt{\beta}\tau_\Omega)^{-1}\sim 1$. The half-width of the former is then smaller than that of the latter by a factor of the order of $\sqrt{\gamma}\tau_\Omega\sim 0.1$. Theoretical frequency-resolved spectra are illustrated on Fig. 5. No experimental work has yet been reported.

B. Discussion

It should be pointed out that the pump-probe absorption of globally charged systems has not yet been systematically examined in the literature. The similarity between signals

resulting from the charge-electric field and dipole-electric field interactions, respectively, is worth noting. However, it survives only if the electric field is spatially constant in a given replica. As expected from the physical grounds, the signal $S(\Omega_1,\Omega_2,\tau)$ does not depend on $\mathbf{r}_0$, the reference point of $\mathbf{M}(\mathbf{r}_0)$. This justifies, *a posteriori*, its choice in the middle of the experimental cell. The computer simulation work generally adheres to this convention.

Another major point is the nonmonotonic behavior of spectral transients and the overshot of an initial bleaching to an induced absorption. It has been under discussion for several years; two proposals have been reported to explain it. According to Kimura *et al.* [9], this effect is due to the transient solvation and local heating following electronic relaxation. On the contrary, Schwartz and Rossky [27] attributed it to a combination of bleaching and absorption dynamics. Our work is in accord with conclusions of Ref. [27]. The data of Graener, Seifert, and Laubereau [52], who measured the time scale of local heating in water, also support them; the latter extends over many picoseconds.

Our work emphasizes the role of the 20-fs dynamics, associated with the reorientational readjustment of water molecules after excitation. A short time scale was also reported in Ref. [27]: nearly 90% of the calculated electronic solvation response is complete within 30 fs of the downward transition. However, the theory predicts this behavior only if the solvation dynamics is fast compared to the laser pulse length, i.e., $\tau_{\Omega 1} \ll \tau_E$. This is why solvation dynamics does not influence the shape of a transient directly. Although very short, the laser pulses should be considered as long in the present case. Entirely different spectra are expected in other circumstances. A growing body of work on aqueous solvation dynamics hints at the same direction [53,54].

The present theory makes several specific predictions, accessible to an experimental check. The temporal width of transients should be different in the wings of the absorption band and around the pump frequency. In addition, the isotope effect, if any, should be present in the wings, but not in the center. The former of these two effects in fact was observed in e^--alcohols [55]; and the absence of isotope effect in the vicinity of the frequency Ω_1 was reported for e^--H_2O [9]. No isobestic point is expected: the presence of the coherent spike precludes its existence. The simple two-state model, proposed by Long, Lu, and Eisenthal [4], is too simple to reproduce the complex spectral behavior.

This discussion may be closed by emphasizing that a satisfactory description of experimental spectra of the hydrated electron was obtained with parameters calculated by *a priori* quantum simulations. This confirms the quality of the latter, the more so as the process under investigation is nonlinear: the existence of several limits is characteristic of these problems. However, it should be stressed that the proper link between experiment and theory can only be established by combining methods of nonlinear statistical mechanics and of quantum simulation. Using one of these two methods alone cannot suffice; a similar conclusion was drawn in other circumstances [56].

ACKNOWLEDGMENTS

The authors wish to thank Professor P. Barbara and Dr. C. Silva for making their results available prior to publication. They also acknowledge gratefully the support of the GDR 1017 of the CNRS and of the Commission of the European Communities. The Laboratoire de Physique Théorique des Liquides is ''Unité de Recherche Associée'' No. 765 at the CNRS.

[1] E. J. Hart and M. Anbar, *The Hydrated Electron* (Wiley, New York, 1970).
[2] L. Kevan and B. C. Webster, *Electron-Solvent and Anion-Solvent Interactions* (Elsevier, Amsterdam, 1970).
[3] A. Migus, Y. Gauduel, J. L. Martin, and A. Antonetti, Phys. Rev. Lett. **58**, 1559 (1987).
[4] F. H. Long, H. Lu, and K. B. Eisenthal, Phys. Rev. Lett. **64**, 1469 (1990).
[5] Y. Gauduel, S. Pommeret, A. Migus, and A. Antonetti, J. Phys. Chem. **95**, 533 (1991).
[6] M. U. Sander, K. Luther, and J. Troe, Ber. Bunsenges. Phys. Chem. **97**, 953 (1993).
[7] J. L. McGowen, H. M. Ajo, J. Z. Zhang, and B. J. Schwartz, Chem. Phys. Lett. **231**, 504 (1994).
[8] J. C. Alfano, P. K. Walhout, Y. Kimura, and P. F. Barbara, J. Chem. Phys. **98**, 5996 (1993).
[9] Y. Kimura, J. C. Alfano, P. K. Walhout, and P. F. Barbara, J. Phys. Chem. **98**, 3450 (1994).
[10] Ph. J. Reid, C. Silva, P. K. Walhout, and P. F. Barbara, Chem. Phys. Lett. **228**, 658 (1994).
[11] D. A. Copeland, N. R. Kestner, and J. Jortner, J. Chem. Phys. **53**, 1189 (1970).
[12] M. D. Newton, J. Phys. Chem. **79**, 2795 (1975).
[13] B. J. Schnitker and P. J. Rossky, J. Chem. Phys. **86**, 3471 (1987).
[14] A. Wallqvist, D. Thirumalai, and B. J. Berne, J. Chem. Phys. **86**, 6404 (1987).
[15] J. Schnitker, K. Motakabbir, P. J. Rossky, and R. Friesner, Phys. Rev. Lett. **60**, 456 (1988).
[16] C. Romero and C. D. Jonah, J. Chem. Phys. **90**, 1877 (1989).
[17] J. Schnitker and P. J. Rossky, J. Phys. Chem. **93**, 6965 (1989).
[18] R. N. Barnett, U. Landman, and A. Nitzan, J. Chem. Phys. **90**, 4413 (1989).
[19] R. N. Barnett, U. Landman, G. Makov, and A. Nitzan, J. Chem. Phys. **93**, 6226 (1990).
[20] E. Neria, A. Nitzan, R. N. Barnett, and U. Landman, Phys. Rev. Lett. **67**, 1011 (1991).
[21] E. Neria and A. Nitzan, J. Chem. Phys. **99**, 1109 (1993).
[22] D. Borgis and A. Staib, Chem. Phys. Lett. **230**, 405 (1994).
[23] A. Staib and D. Borgis, J. Chem. Phys. **103**, 2642 (1995).
[24] F. J. Webster, J. Schnitker, M. S. Friedrichs, R. A. Friesner, and P. J. Rossky, Phys. Rev. Lett. **66**, 3172 (1991).
[25] F. J. Webster, P. J. Rossky, and R. A. Friesner, Comput. Phys. Commun. **63**, 494 (1991).
[26] T. H. Murphey and P. J. Rossky, J. Chem. Phys. **99**, 515 (1993).

[27] B. J. Schwartz and P. J. Rossky, J. Phys. Chem. **98**, 4489 (1994).
[28] B. J. Schwartz and P. J. Rossky, Phys. Rev. Lett. **72**, 3282 (1994).
[29] B. J. Schwartz and P. J. Rossky, J. Chem. Phys. **101**, 6902 (1994).
[30] B. J. Schwartz and P. J. Rossky, J. Chem. Phys. **101**, 6917 (1994).
[31] Y. R. Shen, *The Principles of Nonlinear Optics* (Wiley, New York, 1984).
[32] S. Mukamel, *Principles of Nonlinear Optical Spectroscopy* (Oxford University Press, New York, 1995).
[33] S. Mukamel, Annu. Rev. Phys. Chem. **41**, 647 (1990).
[34] W. T. Pollard, S. Y. Lee, and R. A. Mathies, J. Chem. Phys. **92**, 4012 (1990).
[35] M. J. Rosker, F. W. Wise, and C. L. Tang, Phys. Rev. Lett. **57**, 321 (1986).
[36] S. Bratos and J-Cl. Leicknam, J. Chem. Phys. **101**, 4536 (1994).
[37] S. Bratos and J-Cl. Leicknam, Chem. Phys. Lett. **261**, 117 (1996).
[38] S. Bratos and J-Cl. Leicknam, J. Chem. Phys. **93**, 1737 (1996).
[39] J. H. Weare and I. Oppenheim, Physica (Amsterdam) **72**, 1 (1974).
[40] M. Aihara, Phys. Rev. B **25**, 53 (1982).
[41] R. G. Gordon, Adv. Magn. Reson. **3**, 1 (1968).
[42] A. G. Kofman, R. Zaibel, A. M. Levine, and Y. Prior, Phys. Rev. A **41**, 6434 (1990).
[43] M. Sprik and M. L. Klein, J. Chem. Phys. **89**, 7556 (1988).
[44] M. Sprik, M. L. Klein, and K. Watanabe, J. Phys. Chem. **94**, 6483 (1990).
[45] M. Sprik, J. Phys. Condens. Matter **2**, SA161 (1990).
[46] D. A. V. Kliner, J. C. Alfano, and P. F. Barbara, J. Chem. Phys. **98**, 5375 (1993).
[47] F. Y. Jou and G. R. Freeman, J. Phys. Chem. **83**, 2383 (1979).
[48] D. W. Oxtoby, Adv. Chem. Phys. **47**, 487 (1981).
[49] I. Rips, Chem. Phys. Lett. **245**, 79 (1995).
[50] M. Maroncelli, J. MacInnis, and G. R. Fleming, Science **243**, 1674 (1989).
[51] B. J. Schwartz, E. R. Bittner, O. V. Prezhdo, and P. J. Rossky, J. Chem. Phys. **104**, 5942 (1996).
[52] H. Graener, G. Seifert, and A. Laubereau, Phys. Rev. Lett. **66**, 2092 (1991).
[53] Y. J. Chang and E. W. Castner, J. Chem. Phys. **99**, 7289 (1993).
[54] M. Maroncelli and G. R. Fleming, J. Chem. Phys. **89**, 5044 (1988).
[55] P. K. Walhout, J. C. Alfano, Y. Kimura, C. Silva, P. J. Reid, and P. F. Barbara, Chem. Phys. Lett. **232**, 135 (1995).
[56] S. J. Rosenthal, B. J. Schwartz, and P. J. Rossky, Chem. Phys. Lett. **229**, 443 (1994).